A. V. Moltasov, P. N. Tkacz, S. I. Motrunicz

Effect of Shunting Zone Plastic Strains on Bend Force during the Butt Welding of Rings

Abstract: The article is concerned with the development of an analytical method enabling the calculation of force used for the bending of a ring-shaped product during the butt welding allowing for the presence of plastic strains in the shunting zone. The research involved the investigation of principles governing the plastic-elastic strain of curvilinear bars subjected to bending and the development of theoretical foundations enabling the identification of displacements in such bars. The research-related investigation led to the obtainment of analytical equations combining bend force with movements of welding machine fixing clamps, geometrical parameters and physico-mechanical properties of a ring-shaped product material subjected to welding. Using a number of frames as an example, it was demonstrated that plastic strains significantly affected the value of bend force. The calculation results concerning the volume of bend force obtained using the above named analytical method converged with the results obtained using numerical calculations. Appropriate formulas were used to describe the boundaries of elastic and plastic areas of the shunting zone subjected to bending during butt welding. The research resulted in the determination of the critical value of bending force, the exceeding of which led to the deformation of the required geometrical shape of a ring-shaped product subjected to welding.

Keywords: flash butt welding, ring, shunting zone, plastic strain, bending force

In contrast to open shape products, when calculating the parameters related to the pressure during the butt welding of ring-shaped products it is necessary not only to take into account the cross-sectional area of an element but also to allow for its diameter [1]. This requirement results from the necessity of increasing the welding machine pressure force during flashing and upsetting as well as because of the bending to which the element is subjected [2]. For the first time, the precise computer modelling-aided determination of bending force value was proposed in work [3]. Publication [4] presents the determination of the analytical dependence between the value of bending force and the geometrical parameters of an element subjected to welding.

Tests concerning the stress-strain state of ring-shaped products subjected to butt welding revealed that the shunting zone of the majority of analysed products was characterised by the presence of plastic strains [5] which were

A. V. Moltasov (DSc); P. N. Tkacz (DSc), S. I. Motrunicz (PhD (DSc)) – E.O Paton Electric Welding Institute of the National Academy of Science of Ukraine, Kiev

not allowed for during the calculation of bending force in works [3] and [4]. The above-presented situation inspired the objective of this work, i.e. the determination of the effect of plastic strain in the shunting zone on the value of bending force.
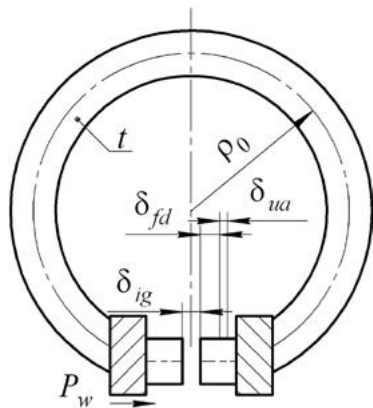
Fig. 1. Diagram presenting the flash butt welding of the ring-shaped product

Computational models are based on the determination the relationship between the movement of welding machine jaws δ_Σ, being the sum of the initial gap width δ_{ig} as well as allowances for flashing δ_{fd} and upsetting δ_{ua} (Fig. 1) and the value of force necessary for overcoming the resistance generated during the bending of the shunting zone. The displacement accompanying the bending of the curvilinear bar was identified using the following formula [6]

$$f_i = \int_{(S)} \left(\frac{1}{\rho} - \frac{1}{\rho_0} \right) \cdot M_i dS \qquad (1)$$

where ρ_0 – radius of bar curvature before deformation; ρ – present radius of bent bar curvature; M_i – formula of the bending moment related to unitary force, the direction of which overlapped with the direction of displacement.

The determination of the displacement required the identification of the dependence between the radius of curvature ρ and the bending moment outside limits of elasticity. To this end, it was necessary to analyse the strain status of the ring segment during bending (Fig. 2).

The linear strain at distance y from the neutral axis of the curvilinear bar was identified using formula [7]

$$\varepsilon = \left(\frac{1}{\rho} - \frac{1}{\rho_0} \right) \cdot y \qquad (2)$$

The linear strain occurred at the furthest points from the neutral axis

$$\varepsilon_{max} = \frac{h \cdot (\rho_0 - \rho)}{2 \cdot \rho_0 \cdot \rho} \qquad (3)$$

where h – height of the ring cross-section.

The dependence of the curvature on the bending moment in the elastic range was linear in nature [8]

$$\frac{1}{\rho} = \frac{M}{EJ} + \frac{1}{\rho_0} \qquad (4)$$

where E – modulus of the longitudinal elasticity of ring material; J – moment of the cross-sectional inertia of the ring determined, according to [9], using the following formula (Fig. 2)

$$J = \frac{b \cdot h^3}{12}$$

where b – ring thickness.

The ring curvature at which the plastic strains started to be generated according to formula (4) was determined using the following formula

$$\frac{1}{\rho_T} = \frac{M_T}{EJ} + \frac{1}{\rho_0} \qquad (5)$$

where M_T – bending moment at which the absolute value of the highest stress at the furthest points from the neutral axis reached the yield point of ring material σ_T. Quantity M_T was determined using the formula of material strength [9]

$$M_T = \frac{\sigma_T \cdot b \cdot h^2}{6} \qquad (6)$$

The strain corresponding to the yield point could be expressed using formulas (2) and (3)

$$\varepsilon_T = \frac{h_T \cdot (\rho_0 - \rho)}{2\rho_0 \cdot \rho} = \frac{h \cdot (\rho_0 - \rho_T)}{2\rho_0 \cdot \rho_T} \qquad (7)$$

where h_T – height of the elastic area (Fig. 2). Then, the use of formulas (3) and (6) led to the

expression

$$\frac{h_T}{h} = \frac{\varepsilon_T}{\varepsilon_{max}} = \frac{\rho \cdot (\rho_0 - \rho_T)}{\rho_T \cdot (\rho_0 - \rho)} \qquad (8)$$

The bending moment in the cross-section was determined using the equilibrium conditions

$$M = 2 \int_0^{h/2} \sigma \cdot b \cdot y \, dy \qquad (9)$$

Expressing y from formula (2), allowing for formula (3) and using it in formula (9) the following formula is obtained:

$$M = \frac{b \cdot h^2}{2\varepsilon_{max}^2} \int_0^{\varepsilon_{max}} \sigma \cdot \varepsilon \, d\varepsilon \qquad (10)$$

Using the schematic diagram of material tension without hardening [10], equation (10) could be presented in the following form:

$$M = \frac{b \cdot h^2}{2\varepsilon_{max}^2} \left[\int_0^{\varepsilon_T} E \cdot \varepsilon^2 d\varepsilon + \int_{\varepsilon_T}^{\varepsilon_{max}} \sigma_T \cdot \varepsilon \, d\varepsilon \right] \qquad (11)$$

After integration and transformations allowing for formulas (6) and (8) it was possible to determine the dependence of bending moment from the curvature in the elastic-plastic area

$$M = \frac{M_T}{2} \left[3 - \left(\frac{\rho \cdot (\rho_0 - \rho_T)}{\rho_T \cdot (\rho_0 - \rho)} \right)^2 \right] \qquad (12)$$

Expressing the curvature from formula (12) allowing for formula (5), the following formula was obtained:

$$\frac{1}{\rho} = \frac{M_T}{EJ \cdot \sqrt{3 - \frac{2M}{M_T}}} + \frac{1}{\rho_0} \qquad (13)$$

Therefore, entering formula (13) to formula (1) it was possible to obtain an expression enabling the identification of displacements in the elastic-plastic area

$$f_i^p = \int_{(S)} \frac{M_T \cdot M_i dS}{EJ \cdot \sqrt{3 - \frac{2M}{M_T}}} \qquad (14)$$
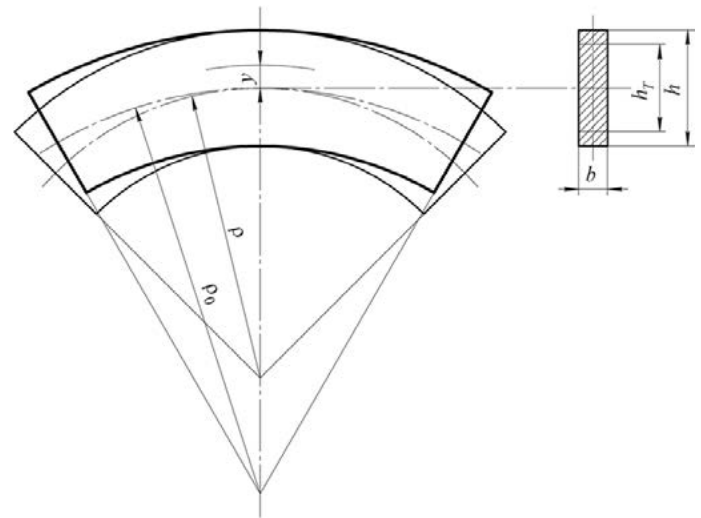
Fig. 2. Change in the curvature of the ring segment subjected to bending

Works [4] and [5] stated that when the ring was subjected to load in accordance with the diagram presented in Figure 1, the diagram of the bending moment related to unitary force applied in the direction of displacement (Fig. 3a) was described by the following formula:

$$M_i = \rho_0 \cdot (1 - \cos\theta) \qquad (15)$$

and the diagram of bending moment forces was described by the following formula:

$$M = -P \cdot \rho_0 \cdot \cos\theta \qquad (16)$$

However, in the case under consideration, the above-presented formula could only be applied in the elastic-linear range, whereas in the elastic-plastic area, the moment would be equal to M_T (Fig. 3b).

Because the diagram of bending moments (Fig. 3b) changed the sign at $\theta = \pm\pi/2$, in cases of any high values of the external load of the ring segment shunting zone appropriate ranges of changes

$$\theta \in [\theta_T ; \pi - \theta_T] \cup [\pi + \theta_T ; 2\pi - \theta_T]$$

would remain elastic and, at the same time, the displacement on these segments would be determined by Mohr integral obtained by using formula (4) in formula (1) [11]

$$f_i^e = \int_{(S)} \frac{M \cdot M_i dS}{EJ} \qquad (17)$$
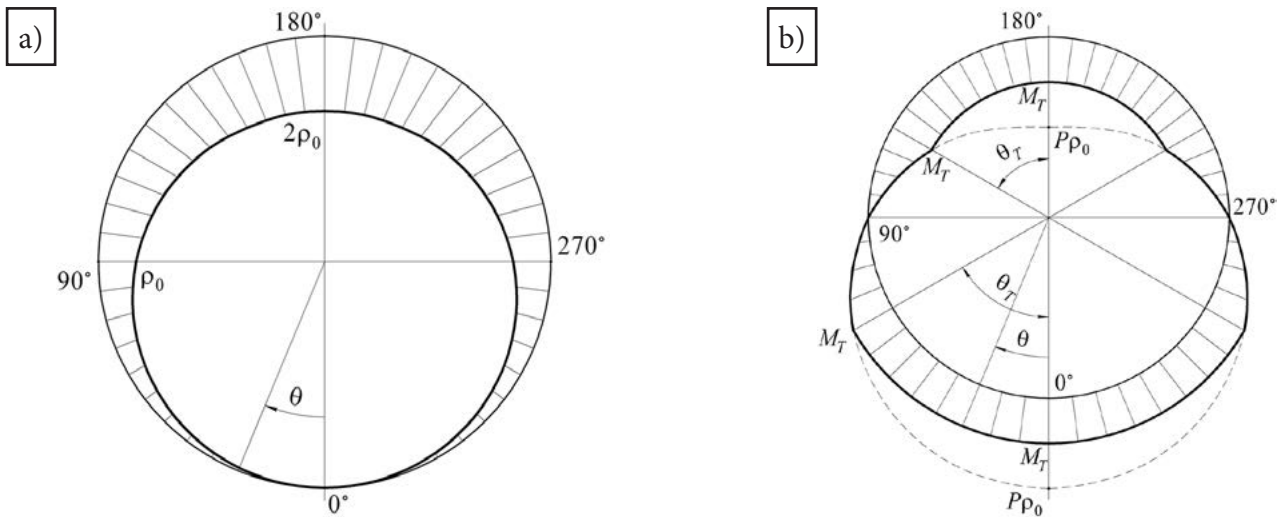
Fig. 3. Diagrams of bending moments: a) of unitary force; b) of applied load (dashed line presents the diagram for ideally elastic material)

Therefore, the movement of welding machine fixing jaws could be calculated by summing integrals (14) and (17), which after allowing for symmetry (Fig. 3) and terms (14) and (15) adopted the following form:

$$\delta_{\Sigma} = \frac{2\rho_0^3}{EJ}\left(\int_0^{\theta_T}\frac{P_T\cdot(\cos\theta-1)d\theta}{\sqrt{3+2\dfrac{P\cdot\cos\theta}{P_T}}} - \int_{\theta_T}^{\pi-\theta_T}P\cdot\cos\theta\cdot(1-\cos\theta)d\theta + \int_{\pi-\theta_T}^{\pi}\frac{P_T\cdot(1-\cos\theta)d\theta}{\sqrt{3+2\dfrac{P\cdot\cos\theta}{P_T}}}\right) \tag{18}$$

where θ_T – circumferential coordinate of the boundary of elastic and elastic-plastic areas (Fig. 3b), identified using the following formula:

$$\theta_T = \arccos\frac{P_T}{P} \tag{19}$$

where P_T – force after the maximum bending moment reached value M_T in accordance with formula (16) and allowing for (6)

$$P_T = \frac{\sigma_T\cdot b\cdot h^2}{6\rho_0} \tag{20}$$

Equation (18) contains elliptical integrals [12] enabling the identification of values which could not be obtained from tables or diagrams [13] because one of the integration boundaries θ_T according to formula (19) depended on force P. As a result, integral equation (18) was solved numerically using the MathCAD software programme for automated designing.

The tests concerning the frames made of steel 12H18N10T involved the calculation of

bending force. It was ascertained that, allowing for plastic strains in the shunting zone, the force amounted to between 53 and 90% of the force value calculated with the assumption of the ideal elasticity of the material (Table 1).

The computational data obtained using the developed analytical method demonstrated the satisfactory convergence with the FEM-based numerical calculation results (Fig. 4); e.g. the maximum deviation of bending force amounted less than 2% (Table 2).
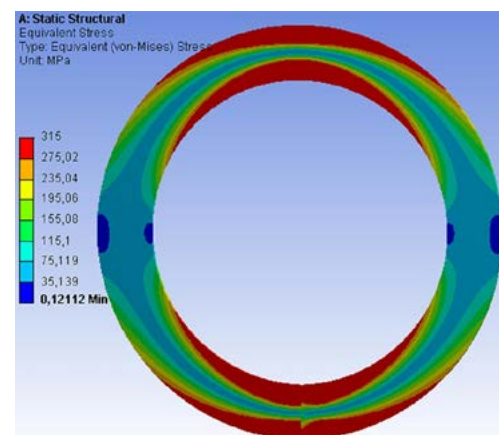
Fig. 4. Field of stresses in the shunting zone of frame no. 3

Table 1. Computational values of bending force during pulsed flash butt welding of frames made of steel 12H18N10T
(σ_T = 315 MPa)

No.	Average radius (ρ_0), mm	Height (h), mm	Thickness (b), mm	Pressure at plasticisation start (P_T), кН	Displacement (δ_Σ), mm	Boundary coordinates (θ_T), °	Plastic bending force (P_B^p), кН	Elastic bending force (P_B^e), кН [4]	P_B^p / P_B^e %
1	185	50	10	7.09	13	45.5	10.12	13.62	74.33
2	205	50	12	7.68	14	43.6	10.61	12.94	82.00
3	301	92	14	20.67	20	46.2	29.85	42.44	70.34
4	283	80	16	19.00	19	45.5	27.10	36.45	74.36
5	296	110	16	34.34	22	47.7	51.07	95.89	53.26
6	195	40	22	9.48	16	43.8	13.13	16.13	81.40
7	198.5	35	25	8.10	16	39.7	10.53	11.64	90.45

Table 2. FEM-based calculation results concerning the bending force during the butt welding of frames

No.	Average radius (ρ_0), mm	Height (h), mm	Thickness (b), mm	Displacement (δ_Σ), mm	Bending force (theoretical), кН	Bending force (MKE), кН	Deviation, %
1	185	50	10	13	10.12	10.20	0.72
2	205	50	12	14	10.61	10.69	0.74
3	301	92	14	20	29.85	29.98	0.42
4	283	80	16	19	27.10	27.25	0.55
5	296	110	16	22	51.07	51.23	0.32
6	195	40	22	16	13.13	13.30	1.30
7	198.5	35	25	16	10.53	10.72	1.81

Using formula (12) to derive the right side of formula (8) and considering formulas (6) and (16), the following equation for the height of the elastic area in various cross-sections of the ring being welded is obtained:

$$h_T = h \cdot \sqrt{3 + 2\frac{P}{P_T}\cos\theta} \qquad (21)$$

The knowledge of the bending force value combined with the use of formulas (19) and (21) made it possible to describe the dimensions and shape of the plasticised zones (Fig. 5). The analysis of equation (21) revealed that in the welded ring cross-sections characterised by the maximum stresses, the elastic area disappeared entirely (Fig. 5) after P reached the value of

$$P_c = \frac{3}{2}P_T \qquad (22)$$

The further increase in the bending force after exceeding the critical value $P > P_c$ would result in the deformation (Fig. 6b) of the geometrical shape of the welded product (Fig. 6a).
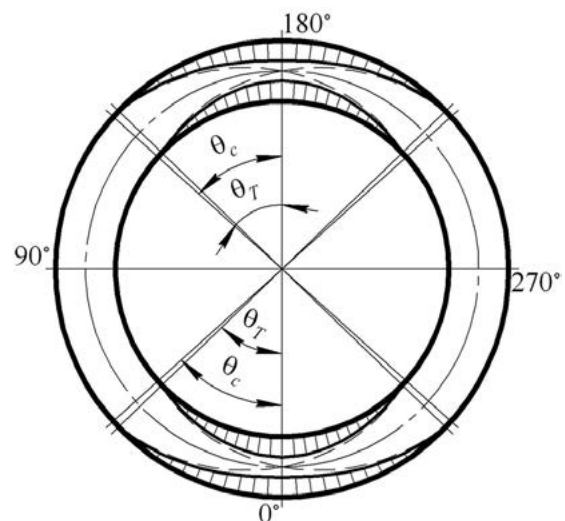
Fig. 5. Plastic areas (pattern) in the shunting zone of frame no. 3 (dashed line presents the boundary of elastic and plastic areas in the boundary state)

The entering of formula (22) to formula (19) enabled the determination of the value of the coordinate of the boundary of the elastic and plastic areas in the boundary state

$$\theta_c = \arccos\frac{2}{3} \qquad (23)$$

The entering of formulas (22) and (23) to formula (18) enabled the determination of the ultimate permissible value of displacement δc which had to be specified when determining allowances, i.e. when selecting the butt welding technology used when joining individual ring-shaped products.

$$\delta_c = \frac{2P_T \cdot \rho_0^3}{EJ}\left(\int_0^{\theta_c}\frac{(\cos\theta-1)\,d\theta}{\sqrt{3+3\cos\theta}} - \frac{3}{2}\int_{\theta_c}^{\pi-\theta_c}\cos\theta\cdot(1-\cos\theta)\,d\theta + \int_{\pi-\theta_c}^{\pi}\frac{(1-\cos\theta)\,d\theta}{\sqrt{3+3\cos\theta}}\right) \qquad (24)$$

Fig. 6. Butt welding of the ring-shaped product: a) element in the K724 welding machine fixing jaws; b) loss of the ring shape by the product

Conclusions

1. By transforming the equations of deformable solid mechanics enabled the identification of the mathematical dependence between the movement of welding machine fixing jaws and force enabling the bending of the element during flash butt welding and allowing for plastic strains in the shunting zone.

2. The calculations of bending force for a number of variously sized frames made of steel 12H18N10T revealed that allowing for plastic strains in the shunting area decreased the value of bending force by 10÷47% in comparison with its value calculated for the case of ideal material elasticity.

3. The reliability of the proposed analytical method was confirmed by slight discrepancies (not exceeding 2%) between the bending force calculation results and the FEM-based numerical results.

4. The obtained mathematical formulas described the boundaries of elastic and plastic areas in the shunting zone subjected to bending during the butt welding of the ring-shaped element. The obtained equations proved that the geometrical shape of the ring-shaped product underwent deformation if bending force was increased to the value being 1.5 times greater than the force corresponding to the initiation of plastic strains in the shunting area. It should be noted that regardless of the geometrical dimensions of the ring-shaped product, the circumferential coordinate of the boundary of elastic and plastic areas is a constant value amounting to ±48.19° and, as a result of symmetry 180°±48.19°.

References

[1] Кочергин К.А. Контактная сварка / К.А. Кочергин // Ленинград: «Машиностроение». – 1987. p. 240 с.: ил.

[2] Кабанов Н.С. Сварка на контактных машинах / Н.С. Кабанов // Учебник для профес.-техн. учебн. заведений. Изд. 2-е, перераб. и доп. – Москва, «Высш. школа». – 1973. – p. 255, с илл.

[3] Лукин М.А. Анализ результатов компьютерного моделирования известных схем деформирования изделий замкнутой формы при стыковой сварке оплавлением / М.А. Лукин, А.И. Самаркин // Вестник ПсковГУ. Серия «Экономические и технические науки». – 2013, no. 3. – pp. 77 – 84.

[4] Чвертко П.Н. Расчёт усилия осадки при контактной стыковой сварке изделий замкнутой формы / П.Н. Чвертко, А.В. Молтасов, С.М. Самотрясов // Автоматическая сварка. – 2014. – no. – pp. 50 – 53.

[5] Молтасов А.В. Разработка методов расчёта силовых параметров контактной стыковой сварки кольцевых изделий: Дис. на здобуття наукового ступеня кандидата техн. наук: 05.03.06; – Захищена 29.12.2015; Затв. 25.02.2016. – Київ, 2015. – p. 132: іл. – Бібліогр.: pp. 119 – 130.

[6] Биргер И.А. Сопротивление материалов: Учебное пособие / И.А. Биргер, Р.Р. Мавлютов // Москва: Наука. Гл. ред. физ.-мат. лит., 1986. – p. 560

[7] Пономарёв С.Д. Расчёты на прочность в машиностроении. Том 2. Некоторые задачи прикладной теории упругости. Расчёты за пределами упругости. Расчёты на ползучесть / С.Д. Пономарёв, В.Л. Бидерман, К.К. Лихарев, В.М. Макушин, Н.Н. Малинин, В.И. Феодосьев // Москва, «Машгиз». – 1958. p. 974

[8] Тимошенко С.П. Сопротивление материалов. Том 1. Элементарная теория и задачи / С.П. Тимошенко // Изд. 2-е, стереотип., Пер. с англ. В.Н. Федорова. – Москва: Наука, 1965. – p. 363

[9] Писаренко Г.С. Опір матеріалів: Підручник / Г.С. Писаренко., О.Л. Квітка, Е.С. Уманський // За ред. Г.С. Писаренка. – 2-ге вид., допов. і переробл. – Київ: Вища шк., 2004. – p. 655: іл.

[10] Малинин Н.Н. Прикладная теория пластичности и ползучести. Учебник для студентов втузов / Н.Н. Малинин // Москва: Машиностроение, 1968, p. 400

[11] Феодосьев В.И. Сопротивление материалов: Учеб. для вузов / В.И. Феодосьев // 10-е изд., перераб. и доп. – Москва: Изд-во МГТУ им. Н.Э. Баумана, 1999, p. 592

[12] Ахиезер Н.И. Элементы теории эллиптических функций / Н.И. Ахиезер // Изд. 2-е, перераб. – Москва: Наука, 1970, p. 304, с илл.

[13] Jahnke E. Tafeln höherer Funktionen / E. Jahnke, F. Emde, F. Lösch // 6, bearbeitete Auflage. – Stuttgart: B.G. Teubner Verlagsgesellschaft, 1960, p. 318